Cell Metabolism
Article

Disrupting the CH1 Domain Structure in the Acetyltransferases CBP and p300 Results in Lean Mice with Increased Metabolic Control

David C. Bedford,[1] Lawryn H. Kasper,[1] Ruoning Wang,[2] Yunchao Chang,[1] Douglas R. Green,[2] and Paul K. Brindle[1,*]
[1]Department of Biochemistry
[2]Department of Immunology
St. Jude Children's Research Hospital, Memphis, TN 38105, USA
*Correspondence: paul.brindle@stjude.org
DOI 10.1016/j.cmet.2011.06.010

SUMMARY

Opposing activities of acetyltransferases and deacetylases help regulate energy balance. Mice heterozygous for the acetyltransferase CREB binding protein (CBP) are lean and insulin sensitized, but how CBP regulates energy homeostasis is unclear. In one model, the main CBP interaction with the glucagon-responsive factor CREB is not limiting for liver gluconeogenesis, whereas a second model posits that Ser436 in the CH1 (TAZ1) domain of CBP is required for insulin and the antidiabetic drug metformin to inhibit CREB-mediated liver gluconeogenesis. Here we show that conditional knockout of *CBP* in liver does not decrease fasting blood glucose or gluconeogenic gene expression, consistent with the first model. However, mice in which the CBP CH1 domain structure is disrupted by deleting residues 342–393 (ΔCH1) are lean and insulin sensitized, as are p300ΔCH1 mutants. $CBP^{\Delta CH1/\Delta CH1}$ mice remain metformin responsive. An intact CH1 domain is thus necessary for normal energy storage, but not for the blood glucose-lowering actions of insulin and metformin.

INTRODUCTION

Energy homeostasis, defined as the balance between energy intake, storage, and expenditure, is regulated in part by energy-sensing sirtuin protein deacetylases (Yu and Auwerx, 2009). Less well understood in the control of energy balance are the roles of protein or histone lysine acetyltransferases (HATs or KATs), which acetylate many metabolic enzymes (Zhao et al., 2010), as well as targets of sirtuin-mediated deacetylation (Hirschey et al., 2010). While it is assumed that the enzymatic activities of HATs are critical for energy balance, the roles of their distinct domains that impart regulatory specificity by binding to transcription factors and other proteins are less clear.

CBP (*Crebbp*) and the closely related p300 (*Ep300*) comprise the KAT3 family of HAT transcriptional coactivators (Allis et al., 2007). Most of the conserved regions of CBP and p300, including those harboring acetyltransferase activity, have little sequence similarity with other HAT families, suggesting that CBP and p300 have unique functions (Bedford et al., 2010; Marmorstein, 2001). Indeed, CBP and p300 are required for normal development, as loss of either one results in early embryonic lethality in mice (Tanaka et al., 1997b; Yao et al., 1998).

Studies of nonlethal mutants have been instructive in determining the role of CBP in later development and physiology. Mice heterozygous for a *CBP* null mutation are growth retarded, as are those heterozygous for an allele that produces a truncated form of CBP (Kung et al., 2000; Oike et al., 1999). The latter mutant has been the more extensively characterized of the two, and it is lean ("lipodystrophic") and more insulin sensitive than wild-type (WT) controls, suggesting that CBP is an important regulator of energy homeostasis (Yamauchi et al., 2002). In this regard, CBP is modeled as central to the counterregulatory effects of glucagon and insulin on gene expression that is required for hepatic gluconeogenesis (He et al., 2009; Yamauchi et al., 2002; Zhou et al., 2004), a critical process for maintaining glucose homeostasis (Biddinger and Kahn, 2006).

During fasting, glucagon produced by the pancreas promotes hepatic glucose production by increasing intracellular cyclic AMP in the liver. Hepatic gluconeogenic gene transcription is stimulated via the recruitment of HAT (CBP/p300) and non-HAT (CRTC) coactivators to the cAMP-responsive transcription factor CREB that is bound to the promoters of target genes (Herzig et al., 2001; Koo et al., 2005). However, mice homozygous for a mutation in CBP that ablates the interaction of CREB and the KIX domain of CBP (Kasper et al., 2002; Xu et al., 2007) have fasting blood glucose levels and hepatic gluconeogenic gene expression that are similar to controls (Koo et al., 2005). This suggests that other domains of CBP besides KIX may be critical for glucose regulation, or that p300 (or the non-HAT CRTC2) can compensate for KIX mutant CBP. Conversely, mice with a serine-to-alanine mutation in the CH1 domain of CBP (Ser436Ala) display increased hepatic gluconeogenic gene expression and increased fasting blood glucose, and are resistant to the hypoglycemia-inducing effects of insulin and metformin (He et al., 2009; Zhou et al., 2004). Since p300 lacks an equivalent serine residue in CH1 (Figure 3A), those studies suggest that CBP has unique insulin- and metformin-responsive properties. Thus, the role of CBP in controlling liver gluconeogenesis is unresolved.

In this study, we inactivated CBP in the liver to further clarify these two models for hepatic gluconeogenesis. Consistent with earlier findings using CBP KIX domain mutant mice, we found

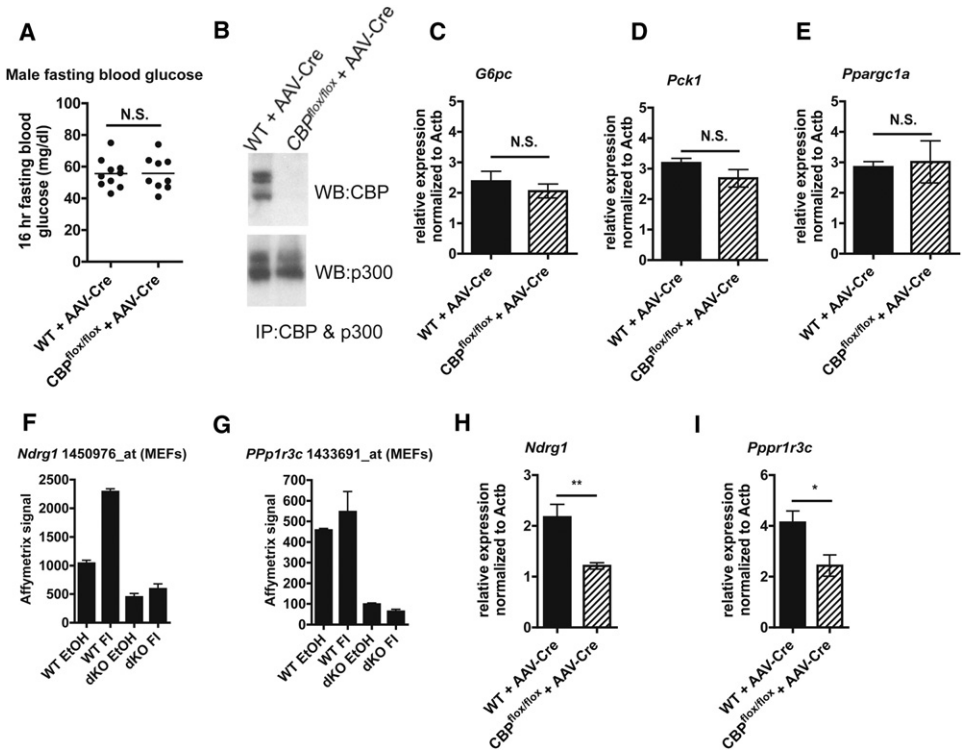

Figure 1. CBP in the Liver Is Not Limiting for Normal Fasting Blood Glucose and Gluconeogenic Gene Expression

(A) Sixteen hour fasting blood glucose in 5-month-old WT and *CBP*$^{flox/flox}$ male mice 7 days after injection with 2.5 × 10^{10} g.c. AAV-Cre (WT + AAV-Cre [n = 10] and *CBP*$^{flox/flox}$ + AAV-Cre [n = 9]).

(B) IP-western of CBP and p300 using liver nuclear extracts.

(C–E) qRT-PCR analysis of mRNA for the indicated hepatic gluconeogenic genes after 16 hr fast (WT + AAV-Cre [n = 10] and *CBP*$^{flox/flox}$ + AAV-Cre [N = 9]).

(F and G) Affymetrix microarray expression signal for the indicated probe sets of *Ndrg1* and *Ppp1r3c* based on mRNA from two independent primary MEF isolates of each genotype (WT and *CBP* and *p300* double null [dKO]); serum-starved MEFs were treated for 90 min with ethanol vehicle (EtOH) or cAMP agonists forskolin + IBMX (FI), n = 2.

(H and I) *Ndrg1* and *Ppp1r3c* expression in the livers of WT + AAV-Cre (n = 10) and *CBP*$^{flox/flox}$ + AAV-Cre (n = 9) fasted male mice. Mean ± SEM. See also Figure S1.

that hepatic CBP does not appear to be limiting for maintaining blood glucose levels. To address whether the CH1 domain is needed for energy homeostasis and the glucose-lowering effects of insulin and metformin, we used mice with germline knockin deletion mutations in CBP and p300 that severely disrupt the structure of the domain. This revealed that the ΔCH1 mutation results in lean mice that respond normally to metformin but have an enhanced insulin response. Together, our findings provide insight into how KAT3 acetyltransferases help maintain energy homeostasis, and suggest that the critical site of action for CBP in regulating glucose homeostasis is outside the liver.

RESULTS

Loss of CBP in the Liver Does Not Significantly Reduce Fasting Blood Glucose or Hepatic Gluconeogenic Gene Expression

Insulin- or metformin-dependent phosphorylation of CBP Ser436 is modeled to disrupt CBP binding to CREB-driven gluconeogenic genes in the liver, thereby repressing their expression and glucose production (He et al., 2009). A different model indicates that CBP is not limiting for liver gluconeogenesis because a mutation in its KIX domain that inhibits binding to CREB does not significantly affect that process (Koo et al., 2005).

To resolve whether CBP in the liver is necessary for glucose homeostasis, we injected *CBP*$^{flox/flox}$ conditional knockout mice (Kang-Decker et al., 2004) with adeno-associated virus that expresses Cre recombinase from a liver-specific promoter (AAV-Cre). The mice were tested 7–18 days after AAV-Cre injection, depending on the assay (see the Experimental Procedures). We found that 16 and 6 hr fasting blood glucose levels were not significantly different between 5-month-old male WT and *CBP*$^{flox/flox}$ mice ($p > 0.05$, Figure 1A, see Figure S1A available online), even though the mutants had markedly reduced levels of CBP in the liver (Figure 1B, Figures S1B and S1C). A replicate experiment using different cohorts of female (6- to 9-month-old) and male (2- to 3-month-old) *CBP*$^{flox/flox}$ mice 7 days after AAV-Cre injection gave similar results for 16 hr fasting blood glucose ($p > 0.05$, Figures S1D and S1E). Glucose tolerance tests (GTTs, to measure the ability of the metabolic tissues to deal with a glucose load), and insulin tolerance tests (ITTs, to determine the glucose lowering effect of bolus i.p. insulin injection) were also not significantly different between WT and *CBP*$^{flox/flox}$ male mice ($p > 0.05$, Figures S1F–S1I).

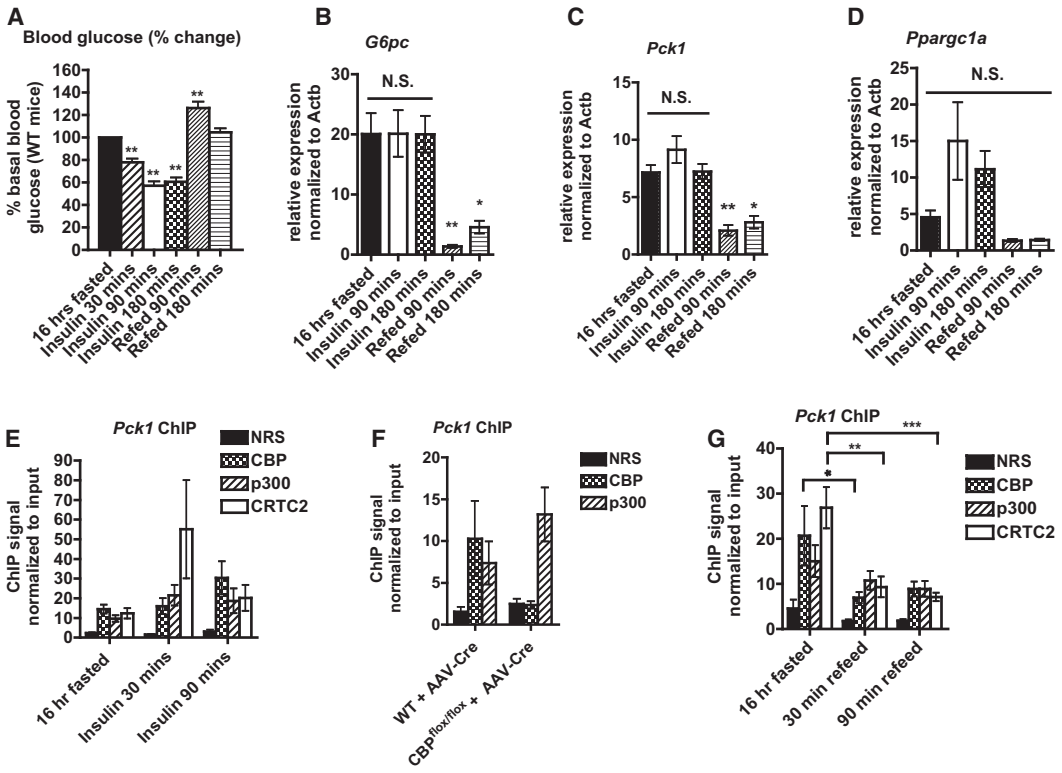

Figure 2. Insulin Injection in Fasted Wild-Type Mice Does Not Rapidly Inhibit the CREB:CBP Complex or Expression of Gluconeogenic Genes in Liver

(A) Compared to fasted WT male mice (n = 23), refeeding for 90′ (n = 4) and 180′ (n = 4) increases blood glucose, whereas insulin (0.5 IU/kg) rapidly lowers blood glucose 30′ (n = 14), 90′ (n = 21), and 180′ (n = 8) after i.p. injection.

(B–D) Fasted (n = 8), insulin-treated (n = 8 for each time point), or refed (n = 4 for each time point) WT mice assayed for hepatic gluconeogenic gene expression; one-way ANOVA with Dunnett's post test was performed to compare each treatment to untreated fasted mice.

(E) ChIP of indicated CREB coactivators at *Pck1* in the livers of fasted WT mice (n = 7 per indicated treatment); normal rabbit serum control (NRS).

(F) CBP and p300 ChIP using livers from fasted mice injected with AAV-Cre (n = 6).

(G) ChIP of CBP, p300, and CRTC2 at *Pck1* in the livers of fasted and refed WT mice; significance of refed versus fasted for the indicated coactivator was determined by ANOVA with Tukey post test (n = 7 mice per indicated treatment). Mean ± SEM. See also Figure S2.

We then used qRT-PCR to measure mRNA in livers from fasted male and female mice. Expression of the gluconeogenic CREB target genes *G6pc* (glucose-6-phosphatase), *Pck1* (PEPCK, phosphoenolpyruvate carboxykinase), and *Ppargc1a* (PGC-1α, a master coregulator of hepatic gluconeogenic gene transcription) were not significantly different from WT animals ($p > 0.05$, male data, Figures 1C–1E, Figures S1M–S1O; female, Figures S1J–S1L). CBP and p300 were expressed at comparable levels in WT liver (Figures S1P–S1R), and in CBP null livers we did not observe evidence for compensation by p300 or other CREB coactivators (i.e., increased expression of *p300*, *Crtc1*, and *Crtc2* mRNAs) ($p > 0.05$, Figures S1S–S1U). Also arguing against complete compensation for the loss of CBP, analysis of the CBP/p300-dependent genes *Ndrg1* and *Ppp1r3c* (Figures 1F and 1G; identified using CBP/p300 double-knockout [dKO] mouse embryonic fibroblasts [MEFs] [Kasper et al., 2010]) revealed they were also repressed in CBP null liver (Figures 1H and 1I). *Ndrg1* was responsive to cAMP in MEFs, suggesting it is a CREB target (Figure 1F). Thus, there are CBP-dependent genes in the liver, but they do not appear to be involved in glucose homeostasis. Together these results show that CBP in the liver is not limiting for gluconeogenic CREB target gene expression or glucose homeostasis. Moreover, since CBP deletion has no significant effect on these processes, it implies that phosphorylation of CBP Ser436 in the liver is also not critical.

Insulin Does Not Rapidly Inhibit the CREB:CBP Complex or Expression of Gluconeogenic Genes in Liver

The lack of a significant effect on glucose homeostasis when hepatic *CBP* was inactivated suggests that insulin does not act by inhibiting CBP binding at CREB target genes in the liver. To further test this idea, we examined whether insulin rapidly inhibits the CREB:CBP complex and CREB-dependent gluconeogenic gene expression. As expected, insulin i.p. injected into WT mice that had been fasted overnight significantly lowered blood glucose after 30, 90, and 180 min (Figure 2A) and increased the phosphorylation of the insulin-responsive kinase AKT in the liver (Figure S2A). However, there was no significant effect upon *G6pc* or *Pck1* mRNA levels 90 and 180 min after insulin injection, whereas *Ppargc1a* mRNA tended to increase at 90 min, albeit with more variability (Figures 2B–2D). A different cohort of mice showed a similar pattern of gene expression after 30 and

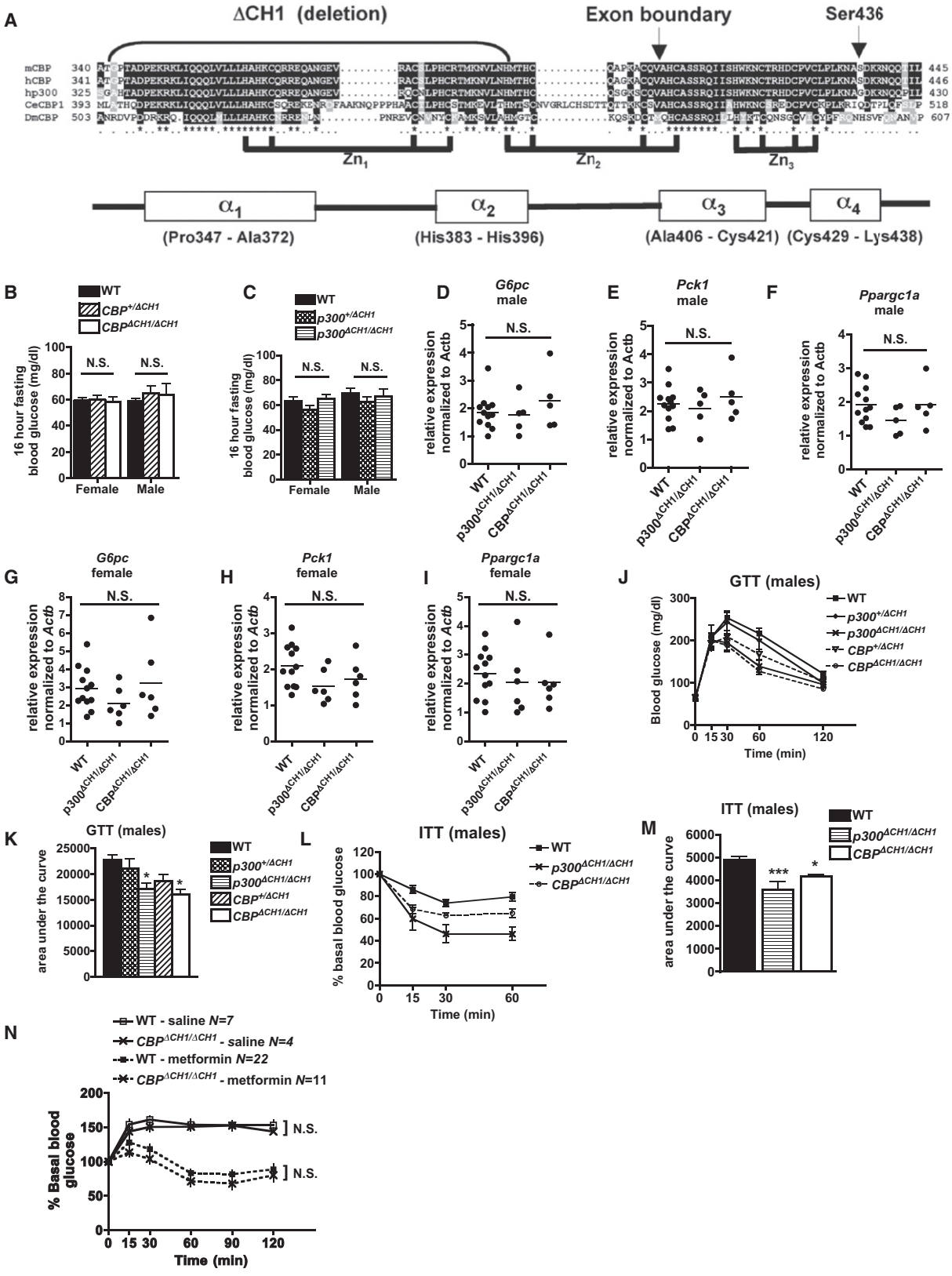

Figure 3. *CBP*$^{\Delta CH1/\Delta CH1}$ and *p300*$^{\Delta CH1/\Delta CH1}$ Mice Have Normal Fasting Blood Glucose Levels but Improved Metabolic Control

(A) CH1 region deleted in *CBP*$^{\Delta CH1}$ and *p300*$^{\Delta CH1}$. Key domain elements are indicated: α helices 1–4 and 12 residues that bind three Zn^{2+} ions; mouse (m), human (h), worm (Ce), fly (Dm).

90 min of insulin (Figures S2B–S2D). As a control for our ability to measure the metabolic regulation of genes in the liver, we examined mRNA levels 90 and 180 min after refeeding (which increases both insulin and satiety hormone release) and observed gene repression (Figures 2B–2D). Thus distinct liver gene expression responses are seen when WT fasted mice are either injected with insulin or refed, a phenomenon also observed by Lipina et al. (Lipina et al., 2005). Tilghman et al. similarly observed that insulin alone does not repress Pck1 protein synthesis in fasted rats (Tilghman et al., 1974). Thus, activating the insulin pathway in the livers of fasted mice is not sufficient to inhibit the expression of *G6pc*, *Pck1*, and *Ppargc1a*. Refeeding therefore appears to modulate the effect of insulin on hepatic gluconeogenic gene expression.

To further test the model of He et al. (He et al., 2009), in which insulin alone disrupts the CREB:CBP complex at hepatic target genes, we performed qPCR chromatin immunoprecipitation (ChIP) on liver tissue from insulin-treated WT mice. This showed that the occurrence of CBP, p300, and CRTC2 (TORC2) at CREB binding sites (CREs) in the *Pck1* promoter was not attenuated by insulin (Figure 2E). The CRTC2 ChIP signal actually increased moderately 30 min after insulin injection. Specificity of the CBP ChIP was confirmed using $CBP^{flox/flox}$ mice injected with AAV-Cre (Figure 2F). CRTC2 and CBP ChIPs were further verified by using antigen-peptide-blocked antibodies (Figure S2E) and showing there was a lack of coactivator enrichment at a region ~20 kb upstream of the *Pck1* promoter CREB binding region (Figure S2F). It therefore appears that insulin alone does not rapidly inhibit the expression of *Pck1* or the binding of CBP at its promoter. Moreover, it seems unlikely that the insulin-dependent phosphorylation of CBP Ser436 in the liver is critical for repressing hepatic CREB target genes.

In contrast to i.p. insulin, refeeding for 30 or 90 min attenuated the ChIP signals for all three coactivators (CBP, p300, and CRTC2) at the *Pck1* promoter (Figure 2G), consistent with the reduced expression of *Pck1* in response to refeeding(Figure 2C). This suggests two things: (1) refeeding and insulin injection are not equivalent for disrupting CREB coactivator complex formation and inhibiting transcription, and (2) the recruitment of multiple coactivators must be inhibited to repress hepatic gluconeogenic gene expression, which agrees with our results using CBP liver knockout mice.

The ΔCH1 Mutation in CBP and p300 Removes Critical CH1 Domain Components

Although our data indicate that CBP in the liver is not essential for glucose homeostasis, mice heterozygous for a *CBP* germline mutation that truncates at aa 1084 (deleting 1357 residues) are lean and insulin sensitive (Yamauchi et al., 2002). The CBP functional deficiencies that lead to this phenotype are unclear, however. One clue was provided by a report that the CH1 domain of CBP is important for transactivation in response to insulin (Zanger et al., 2001). In addition, a S436A germline mutation in *CBP* causes an insulin-resistant phenotype (Zhou et al., 2004), suggesting that it is the CH1 domain that is important for metabolic control.

We tested this idea by using mice carrying deletions in one of the two exons that encode the CH1 (TAZ1) domain of CBP ($CBP^{\Delta CH1}$) and p300 ($p300^{\Delta CH1}$) (Kasper et al., 2005). The deletion mutations are essentially equivalent in CBP and p300 (aa 342–393 deleted for CBP, and 329–379 for p300), and remove two of the domain's four α helices, five Cys and His residues that bind two of the three zinc ions in the structure, 8 of 14 residues that form the conserved hydrophobic core, and much of the binding surface for HIF-1α and CITED2 (Dames et al., 2002; De Guzman et al., 2004; Freedman et al., 2002, 2003) (Figure 3A, Figure S3A). The hydrophobic core and binding of zinc are essential for the structural integrity of the CH1 domain (Gu et al., 2001; Matt et al., 2004; Newton et al., 2000), indicating that the ΔCH1 mutation will inhibit the interaction with most, if not all, CH1-binding partners. Ser436 is part of the extended CBP CH1 α4 helix that is not removed by the ΔCH1 mutation (Figure 3A, Figure S3A), although interactions between α4 and the hydrophobic core of the domain are disrupted by the deletion of helices α1 and α2 (De Guzman et al., 2004). Thus, whether the hypoglycemic effects of insulin or metformin require an intact CH1 structure can be addressed using these mice.

Improved Glucose Tolerance and Insulin Sensitivity in $CBP^{\Delta CH1/\Delta CH1}$ and $p300^{\Delta CH1/\Delta CH1}$ Mice

We tested whether fasting blood glucose is affected in $CBP^{\Delta CH1/\Delta CH1}$ mice but found no significant effect compared to controls ($p > 0.05$, Figure 3B). A similar result was obtained using $p300^{\Delta CH1/\Delta CH1}$ mice ($p > 0.05$, Figure 3C). In agreement with the fasting glucose results, hepatic gluconeogenic gene expression was not significantly altered in fasted $p300^{\Delta CH1/\Delta CH1}$ and $CBP^{\Delta CH1/\Delta CH1}$ mice (2- to 3-month-old males, Figures 3D–3F; 2- to 5-month-old females, Figures 3G–3I). Interestingly, some, but not all, 8- to 10-month-old male $CBP^{\Delta CH1/\Delta CH1}$ mice showed elevated expression of *G6pc*, *Pck1*, and *Ppargc1a* in the liver, although fasting blood glucose was not significantly different from age-matched WT and $p300^{\Delta CH1/\Delta CH1}$ mice (Figures S3B–S3E). Comparing our results from the different age cohorts suggests that variable gluconeogenic gene expression among older $CBP^{\Delta CH1/\Delta CH1}$ mutants reflects an indirect effect of their physiological status rather than a direct action of

(B and C) Sixteen hour fasting blood glucose in $CBP^{\Delta CH1/\Delta CH1}$ and $p300^{\Delta CH1/\Delta CH1}$ mice and controls (B, male WT [n = 18], $CBP^{+/\Delta CH1}$ [n = 14], $CBP^{\Delta CH1/\Delta CH1}$ [n = 7]; female WT [n = 14], $CBP^{+/\Delta CH1}$ [n = 11], $CBP^{\Delta CH1/\Delta CH1}$ [n = 11]; and C, male WT [n = 13], $p300^{+/\Delta CH1}$ [n = 12], $p300^{\Delta CH1/\Delta CH1}$ [n = 10]; female WT [n = 15], $p300^{+/\Delta CH1}$ [n = 9], $p300^{\Delta CH1/\Delta CH1}$ [n = 12]).
(D–I) qRT-PCR analysis of mRNA for the indicated hepatic gluconeogenic genes after 16 hr fast for 2- to 3-month-old males (D–F) and 2- to 5-month-old females (G–I); each dot represents a biological replicate, mean value indicated.
(J) GTT for indicated male ΔCH1 mutants and controls; WT (n = 31), $p300^{+/\Delta CH1}$ (n = 12), $p300^{\Delta CH1/\Delta CH1}$ (n = 10), $CBP^{+/\Delta CH1}$ (n = 19), $CBP^{\Delta CH1/\Delta CH1}$ (n = 9).
(K) AUC analysis of GTT data shown in (J).
(L) ITT of WT (n = 28), $CBP^{\Delta CH1/\Delta CH1}$ (n = 9), and $p300^{\Delta CH1/\Delta CH1}$ (n = 8) mice.
(M) AUC analysis of ITT data shown in (L).
(N) MTT for WT and $CBP^{\Delta CH1/\Delta CH1}$ mice at 4–6 months of age; sample sizes indicated. Fasting blood glucose and GTT analyses were performed at 15 weeks of age and ITTs at 6–8 months of age. Mean ± SEM. See also Figure S3.

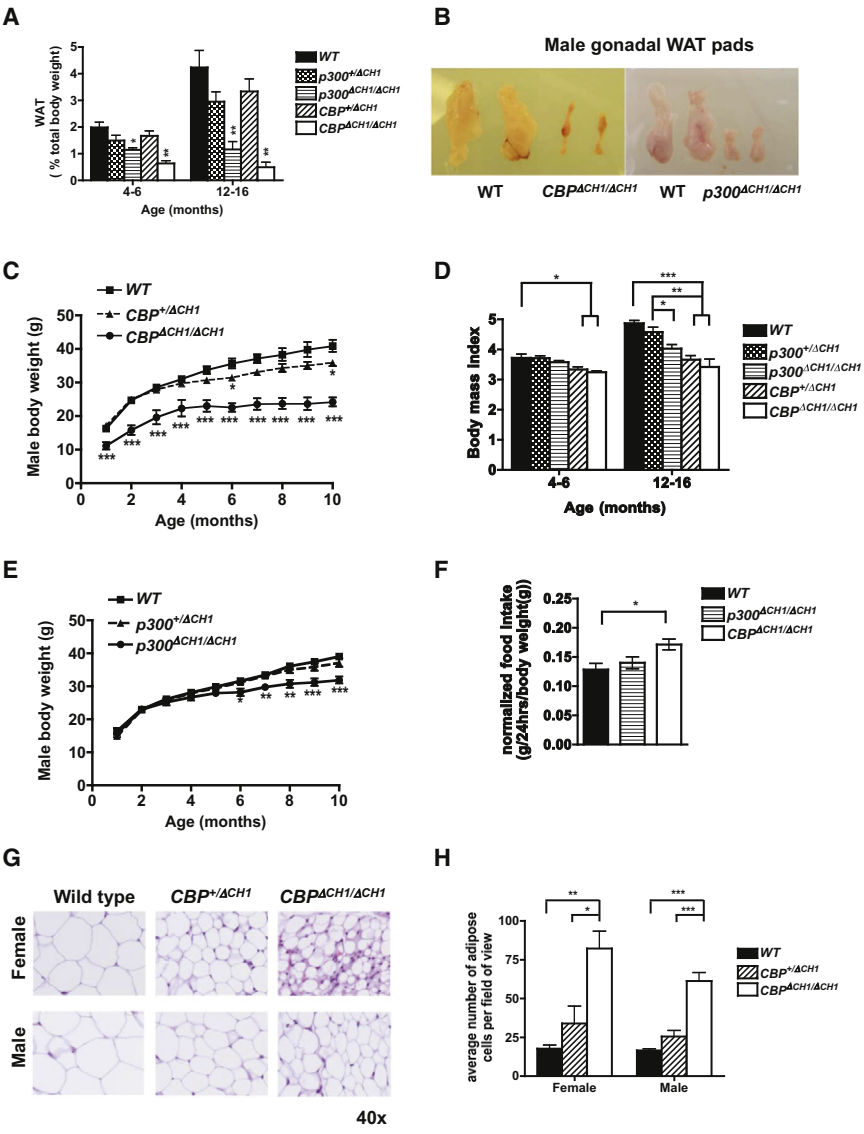

Figure 4. $CBP^{\Delta CH1/\Delta CH1}$ and $p300^{\Delta CH1/\Delta CH1}$ Mice Have Reduced WAT and Body Mass

(A) Male WAT as a percentage of total body weight for genotypes and ages indicated (n = 5–21).

(B) Male gonadal WAT pads at 12 months of age (right and left pads shown).

(C) Body weight profiles for male CBP ΔCH1 mice (at least seven mice per genotype).

(D) BMI for male $CBP^{\Delta CH1/\Delta CH1}$ and $p300^{\Delta CH1/\Delta CH1}$ mice at indicated ages (n = 5–19).

(E) Body weight profiles for male p300ΔCH1 mice (at least ten mice per genotype).

(F) Average daily food intake normalized to total body weight for WT (n = 18), $p300^{\Delta CH1/\Delta CH1}$ (n = 7), and $CBP^{\Delta CH1/\Delta CH1}$ (n = 9) male mice at 4–8 months of age.

(G) H&E stain of gonadal WAT pads.

(H) Quantification of average number of cells per field of view in WAT pad sections WT (n = 3), $CBP^{+/\Delta CH1}$ (n = 4), $CBP^{\Delta CH1/\Delta CH1}$ (n = 3). Mean ± SEM. See also Figure S4.

the CBP ΔCH1 protein on liver target genes. Nonetheless, severe disruption of the CBP or p300 CH1 domain structure in every tissue of the mouse does not affect fasting blood glucose, expanding upon the result obtained with conditional knockout of *CBP* in liver.

We next performed GTTs, as *CBP* S436A mutant mice are glucose intolerant and insulin resistant (Zhou et al., 2004), while mice heterozygous for a truncated allele of CBP (retaining CH1 but lacking the HAT domain) have increased glucose tolerance and insulin responsiveness (Yamauchi et al., 2002). In contrast to *CBP* S436A mutants, $CBP^{\Delta CH1/\Delta CH1}$ and $p300^{\Delta CH1/\Delta CH1}$ mice showed improved glucose tolerance relative to WT animals ($p < 0.05$, Figures 3J and 3K). Improved glucose tolerance in the ΔCH1 mutants indicates insulin sensitization, so we performed ITTs. $CBP^{\Delta CH1/\Delta CH1}$ ($p < 0.05$) and $p300^{\Delta CH1/\Delta CH1}$ ($p < 0.001$) mice both showed an enhanced ability to lower blood glucose in response to insulin, indicating that their improved glucose responsiveness was due to increased insulin sensitivity (Figures 3L and 3M). As CBP liver knockout mice had normal ITT and GTT responses (Figure S1F–S1I), these results indicate that the CH1 domain of CBP and p300 is critical outside the liver for glucose homeostasis. Speculating, it might be that the CBP truncation (Yamauchi et al., 2002) and ΔCH1 mutations similarly affect these physiological functions via related mechanisms (e.g., inhibiting the activity of a CH1-binding transcription factor).

$CBP^{\Delta CH1/\Delta CH1}$ Mice Lower Their Blood Glucose Normally in Response to the Antidiabetic Drug Metformin

The CBP CH1 structural domain could be inferred to mediate the glucose-lowering effect of metformin that occurs in response to Ser436 phosphorylation (He et al., 2009). To examine this, we performed metformin tolerance tests (MTTs). This showed that i.p. metformin lowered fasting blood glucose levels similarly in WT and $CBP^{\Delta CH1/\Delta CH1}$ mice ($p > 0.05$) when compared to i.p. saline (Figure 3N). Thus, disrupting the CH1 domain structure of CBP enhances insulin sensitivity, but it does not affect the blood glucose-lowering action of metformin.

$CBP^{\Delta CH1/\Delta CH1}$ and $p300^{\Delta CH1/\Delta CH1}$ Mice Have Reduced Body Weight and White Adipose Tissue

Increased insulin responsiveness suggests enhanced metabolic control. In line with this, $CBP^{\Delta CH1/\Delta CH1}$ and $p300^{\Delta CH1/\Delta CH1}$ mice at 4–16 months of age had significantly reduced white adipose tissue (WAT) as a percentage of body weight, which became more apparent with age (male data, Figures 4A and 4B; female data, Figures S4A–S4C).

Consistent with reduced WAT, $CBP^{\Delta CH1/\Delta CH1}$ mice weighed less than same sex controls at all ages (males, Figure 4C; females,

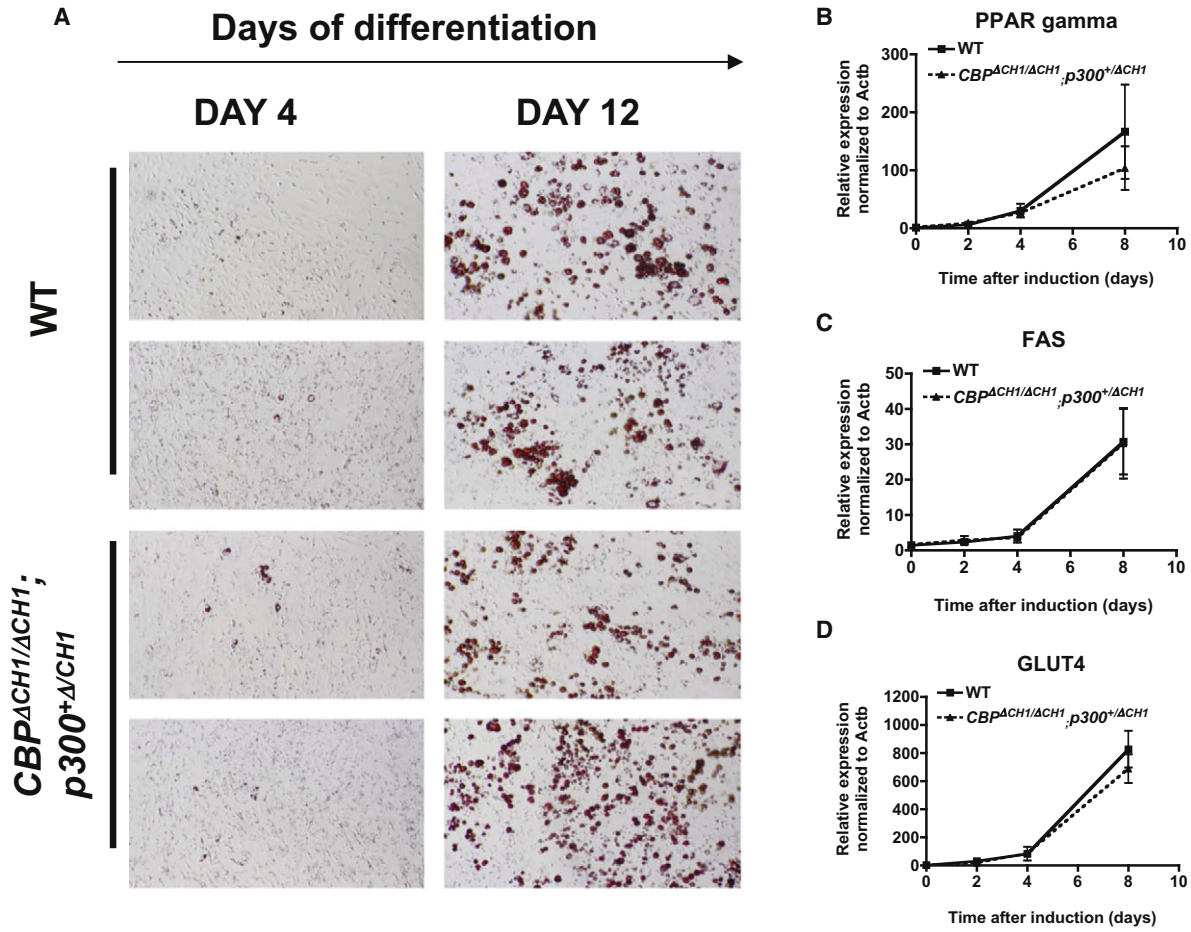

Figure 5. $CBP^{\Delta CH1/\Delta CH1}$;$p300^{+/\Delta CH1}$ and WT MEFs Differentiate Comparably into Adipocytes

(A) Oil red O staining of WT and $CBP^{\Delta CH1/\Delta CH1}$;$p300^{+/\Delta CH1}$ MEFs cultured for 4 or 12 days in adipocyte-differentiation media. Two independent primary MEF isolates of each genotype are shown.

(B–D) mRNA levels of adipogenic gene markers PPAR-gamma (*Pparg*), FAS (*Fasn*), and glucose transporter 4 (GLUT4, *Slc2a4*) during the first 8 days of differentiation. n = 2 independent MEF isolates per genotype. Mean ± SEM. See also Figure S5.

Figure S4D). Although growth retardation of $CBP^{\Delta CH1/\Delta CH1}$ mice accounted for part of their reduced weight, they had a lower body mass index (BMI) than WT mice as early as 4–6 months of age (Figure 4D), indicating that their reduced weight was not solely due to their smaller size. $CBP^{+/\Delta CH1}$ mice showed an intermediate phenotype for body weight and BMI, especially as they aged (Figures 4C and 4D, Figure S4D). $p300^{\Delta CH1/\Delta CH1}$ mice were not growth retarded, yet they also exhibited lower body weight (Figure 4E, males; Figure S4E, females) and reduced BMI (Figure 4D). WT, $CBP^{\Delta CH1/\Delta CH1}$, and $p300^{\Delta CH1/\Delta CH1}$ mice consumed similar amounts of normal chow (data not shown), although $CBP^{\Delta CH1/\Delta CH1}$ mutants ate more in comparison to their body weight ($p < 0.05$, Figure 4F). This indicates the reduced BMI of the ΔCH1 mutants is not due to decreased food intake. Thermogenic brown adipose tissue (BAT) might be expected to be more abundant in lean animals, but it was actually reduced in 10- to 12-month-old $CBP^{\Delta CH1/\Delta CH1}$ mice relative to WT, although this difference was not significant when normalized to body weight ($p > 0.05$, Figures S4F and S4G).

WAT Adipocytes from $CBP^{\Delta CH1/\Delta CH1}$ Mice Are Smaller

The reduced WAT mass in ΔCH1 mutant mice could be caused by fewer or smaller fat cells. Histological analysis of gonadal WAT from 4- to 6-month-old $CBP^{\Delta CH1/\Delta CH1}$ mice showed that adipocytes were smaller compared to controls ($p < 0.05$, Figures 4G and 4H). To help determine if the ΔCH1 mutation inhibits fat synthesis or storage, we differentiated WT and $CBP^{\Delta CH1/\Delta CH1}$;$p300^{+/\Delta CH1}$ MEFs into adipocytes ex vivo. These mutant adipocytes were severely deficient for normal CH1 domains, but they did not obviously differ from WT cells, as shown by oil red O staining for lipids and the expression of adipogenic marker genes encoding peroxisome proliferator-activated receptor gamma (PPAR gamma, *Pparg*), fatty acid synthase (FAS, *Fasn*), and glucose transporter-4 (GLUT4, *Slc2a4*) (Figure 5). Consistent with these in vitro findings, expression of the fatty acid storage and metabolism genes *Plin2*, *Fabp4*, *Fabp5*, *Plin1*, *Cpt1b*, and *Acaca* in WAT isolated from 8- to 10-month-old WT, $CBP^{\Delta CH1/\Delta CH1}$, and $p300^{\Delta CH1/\Delta CH1}$ mice was comparable ($p > 0.05$, Figures S5A–S5F). In addition, fatty acid oxidation measurements (Brivet et al., 1995; Buzzai

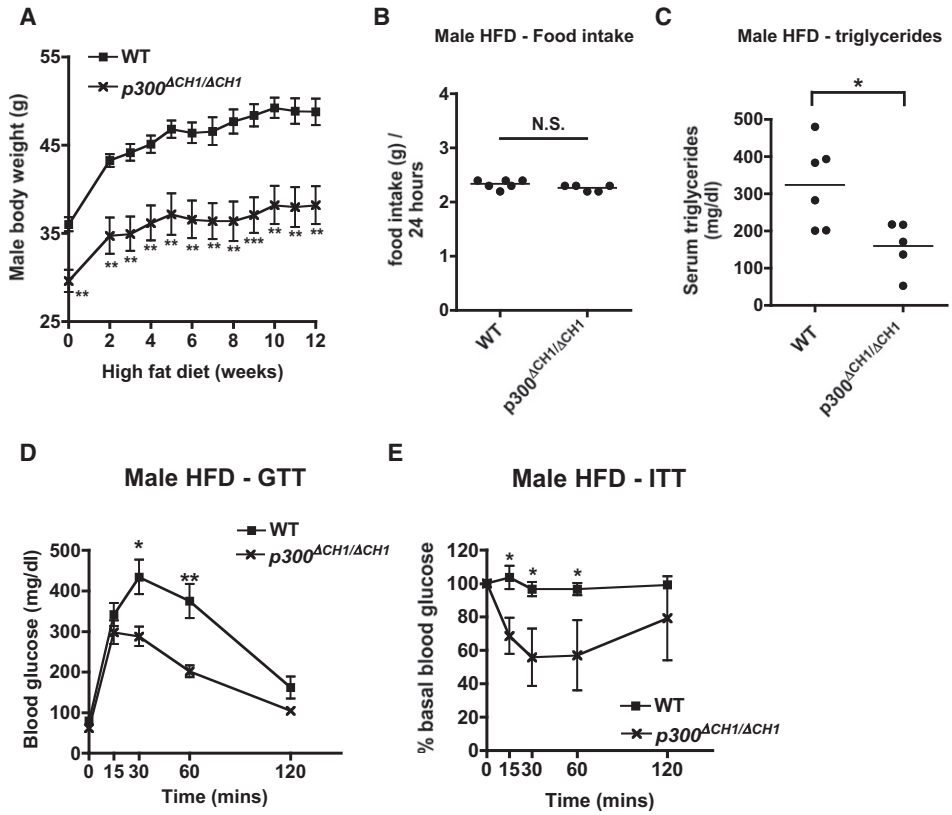

Figure 6. $p300^{\Delta CH1/\Delta CH1}$ Mice on a High-Fat Diet Have Improved Serum Triglycerides, Glucose Tolerance, and Insulin Sensitivity Compared to WT Littermates

(A) Body weights of 10- to 12-month-old WT (n = 6) and $p300^{\Delta CH1/\Delta CH1}$ (n = 5) male mice on a HFD for 12 weeks.

(B) Food intake between HFD weeks 11 and 12.

(C) Serum triglyceride levels of male mice fed the HFD for 12 weeks.

(D) GTT data obtained for WT (n = 5) and $p300^{\Delta CH1/\Delta CH1}$ (n = 5) after 10 weeks on the HFD.

(E) ITT data for WT (n = 6) and $p300^{\Delta CH1/\Delta CH1}$ (n = 3) mice after 12 weeks of HFD. Mean ± SEM.

et al., 2005) using adipocytes isolated from WAT were not obviously different between WT and mutants when normalized to nuclear DNA, which is indicative of cell number (Figures S5G and S5H; Figure 4G shows that the mutant adipocytes are smaller and thus more abundant on a tissue weight basis). These results together suggest that reduced WAT mass in ΔCH1 mutant mice is caused by altered energy demand or storage, rather than abnormal adipogenesis or adipocyte fatty acid metabolism.

$p300^{\Delta CH1/\Delta CH1}$ Mice Are Resistant to the Adverse Metabolic Consequences of a High-Fat Diet

The enhanced metabolic control observed in ΔCH1 mutant mice fed a normal chow diet suggested that they would be more resistant to the deleterious effects of a high-fat diet (HFD). We tested this idea using 10- to 12-month-old $p300^{\Delta CH1/\Delta CH1}$ male mice. At this age, the mutants started out relatively lean, yet after 12 weeks of HFD they still weighed significantly less than HFD WT animals, despite similar food intake (Figures 6A and 6B). Moreover, $p300^{\Delta CH1/\Delta CH1}$ mice showed resistance to HFD-induced elevated serum triglycerides, glucose intolerance, and insulin resistance when compared to WT controls ($p < 0.05$, Figures 6C–6E). Together, these findings suggest that reducing CH1 functionality increases metabolic control with both normal diets and HFDs.

DISCUSSION

Using a tissue-specific conditional knockout of *CBP*, we demonstrated that this HAT is not limiting in the liver for glucose homeostasis or hepatic gluconeogenic gene expression. However, germline mutations in *CBP* and *p300* that severely disrupt the structure of CH1 showed that this domain is critical for maintaining fat reserves, although it is not limiting for the blood glucose-lowering activities of insulin and metformin. Consistent with their lean phenotype, both $CBP^{\Delta CH1/\Delta CH1}$ and $p300^{\Delta CH1/\Delta CH1}$ mice were insulin sensitized, showing that disrupting the CH1 domain improves metabolic control in vivo. And for CBP at least, the critical organ system(s) for regulating glucose homeostasis appears to be outside the liver. Thus, identifying the transcription factor-binding CH1 domain as a key component of a metabolic regulatory pathway provides mechanistic insight into how CBP and p300 modulate energy homeostasis.

The CH1 domain is one of the few regions of a mammalian HAT to have been analyzed in vivo using more than one knockin

mutation (i.e., ΔCH1 and S436A mice). Our findings therefore help reveal how this domain controls energy homeostasis, a topic relevant to the expanding roles ascribed to acetyltransferases in metabolism (Feige and Auwerx, 2007; Zhao et al., 2010), and the fact that CBP and p300 act as regulatory network "hubs" (they have more than 400 described protein interaction partners) (Bedford et al., 2010). With regard to CH1-binding partners, hypoxia-inducible factor 1α (HIF-1α), which requires the CH1 domain for its full transactivation activity (Kasper et al., 2005; Kasper and Brindle, 2006), affects adipose tissue in complex ways (Halberg et al., 2009; Zhang et al., 2010), but the expression of HIF target genes *Edn1*, *Higd1a*, *Slc2a1* (GLUT1), and *Vegfa* (VEGF) was not repressed in WAT directly isolated from $CBP^{\Delta CH1/\Delta CH1}$ and $p300^{\Delta CH1/\Delta CH1}$ mice (data not shown). Additionally, identifying the CH1 domain as a mediator of the metabolic functions of CBP helps clarify prior findings that implicated CBP in both insulin-sensitized (Yamauchi et al., 2002) and insulin-resistant phenotypes (He et al., 2009). The similar metabolic phenotype we observe with both $CBP^{\Delta CH1/\Delta CH1}$ and $p300^{\Delta CH1/\Delta CH1}$ mice argues that the role for the CH1 domain in energy homeostasis is not specific to only one member of the KAT3 family.

The ΔCH1 mutation does not remove Ser436 in CBP, but the differences between the CBPΔCH1 and S436A phenotypes are not inconsistent if the ΔCH1 mutation acts independently of Ser436 phosphorylation. A role for the CH1 domain in metabolic control that is independent of Ser436 is supported by the similarities of the metabolic phenotypes of $CBP^{\Delta CH1/\Delta CH1}$ and $p300^{\Delta CH1/\Delta CH1}$ mice even though p300 CH1 has a glycine at the position comparable to Ser436. If, for example, Ser436 phosphorylation in response to insulin inhibits CBP CH1 domain function, then the ΔCH1 mutation might have mimicked the effect of this phosphorylation and promoted fasting hypoglycemia. We did not see this, however, as $CBP^{\Delta CH1/\Delta CH1}$ mice had normal fasting blood glucose levels, although they did have an enhanced response to injected glucose or insulin. On the other hand, if the ΔCH1 mutation prevents Ser436 phosphorylation or disrupts the ability of phospho-Ser436 to activate CH1 (or other CBP domains or binding partners), then one might expect $CBP^{\Delta CH1/\Delta CH1}$ mice to be insulin resistant like S436A mutants, which they are not. Alternatively, the CH1 domain and Ser436 may act by independent physiological pathways. In support of the latter model, the glucose-lowering activity of metformin was not affected by the CBP ΔCH1 mutation, which also suggests that this drug works differently from insulin. It is important to reemphasize, however, that loss of CBP in the liver had no measurable effect on glucose homeostasis, indicating that the phosphorylation of hepatic CBP Ser436 is not physiologically relevant for that function.

Indeed, several of our findings are inconsistent with the model in which CBP Ser436 phosphorylation by insulin-stimulated PKCι/λ inhibits CREB:CBP complex formation at gluconeogenic genes in the liver, thereby reducing gluconeogenesis and blood glucose levels (He et al., 2009; Zhou et al., 2004).

First, in contrast to a fast/refeed paradigm, we did not observe an obvious and sustained decrease in gluconeogenic gene mRNA levels in the livers of fasted WT mice injected with insulin. Nor did we observe an insulin-dependent loss of CBP recruitment to such genes. It is possible that our failure to observe these phenomena was due to experimental conditions (e.g., mouse strain) or approach (e.g., euglycemia was not maintained). Nevertheless, a reduction in gluconeogenic gene expression would seem unlikely to contribute substantially to an acute reduction in blood glucose in response to insulin. In this regard, Ramnanan et al. have shown that reduced hepatic glucose output in response to acute hyperinsulinemia in euglycemic fasted canines is mostly due to changes in glycolysis and glycogen synthesis rather than the repression of gluconeogenesis via downregulation of *Pck1* expression (Ramnanan et al., 2010).

Second, we showed that conditional knockout of CBP in the liver did not significantly affect fasting blood glucose levels or gluconeogenic gene expression. It is possible that using different methods to reduce liver CBP (e.g., RNAi versus knockout) might lead to different phenotypes, but the knockout data are consistent with a model in which CBP in the liver is not limiting for glucose homeostasis.

Third, we found that PKC iota (PKCι, PKCι/λ, PKCλ), which is modeled as the insulin-responsive CBP Ser436 kinase in liver (He et al., 2009), does not measurably phosphorylate Ser436 in vitro. Using purified recombinant PKCι (Promega), we did not observe evidence for significant inducible Ser436 phosphorylation with the following substrates: (1) WT, ΔCH1, S436A, and ΔCH1/S436A CBP-HA proteins expressed in 293T cells and immunoprecipitated with anti-HA antibody (Figures 7A and 7B); (2) a synthetic CBP 430–442 peptide (LPLKNASDKRNQQ) (Figure 7C); (3) endogenous CBP immunoprecipitated from extracts prepared from serum-starved and insulin-treated HepG2 cells (Figure S6A); (4) endogenous CBP immunoprecipitated from liver nuclear extracts prepared from fasted WT mice (Figure S6B); (5) dual-affinity purified full-length GST-CBP-310-452-FLAG proteins (WT, ΔCH1, S436A, and ΔCH1/S436A mutants) produced in *E. coli* (Figures S6C and S6D). Importantly, in each assay, PKCι was able to efficiently phosphorylate itself and other substrates (e.g., FLAG-CREB, GST-CREM, CREBtide), but not CBP Ser436. The inability of PKCι to phosphorylate CBP S436 in vitro might be explained by the findings of Fujii et al., who showed that Asp at the +1 position relative to Ser strongly disfavors phosphorylation by PKC, consistent with the basophilic nature of this kinase family (Fujii et al., 2004). Together, these results indicate that if CBP Ser436 is phosphorylated in response to insulin, it is probably not by PKCι. Moreover, Matsumoto et al. showed that the conditional knockout of PKC iota (also called PKC lambda) in the liver increases insulin sensitivity, and not *Pck1* and *G6pc* expression, further suggesting this kinase does not repress gluconeogenic genes in the liver by phosphorylating CBP Ser436 (Matsumoto et al., 2003).

The normal fasting blood glucose levels seen in $CBP^{\Delta CH1/\Delta CH1}$ mice agreed well with the unchanged hepatic gluconeogenic gene expression and fasting blood glucose we observed in mice deficient in liver CBP, as well as previously published data on $CBP^{KIX/KIX}$ mice (Koo et al., 2005). This suggests other coactivators in the liver besides CBP provide redundant coactivation function for hepatic gluconeogenesis even though CBP is limiting for the expression of other genes in that organ (e.g., *Ndrg1*, *Pppr1c3*). This is consistent with the notion that individual CREB target genes dictate and utilize different coactivator mechanisms for their expression in response to cAMP (Kasper

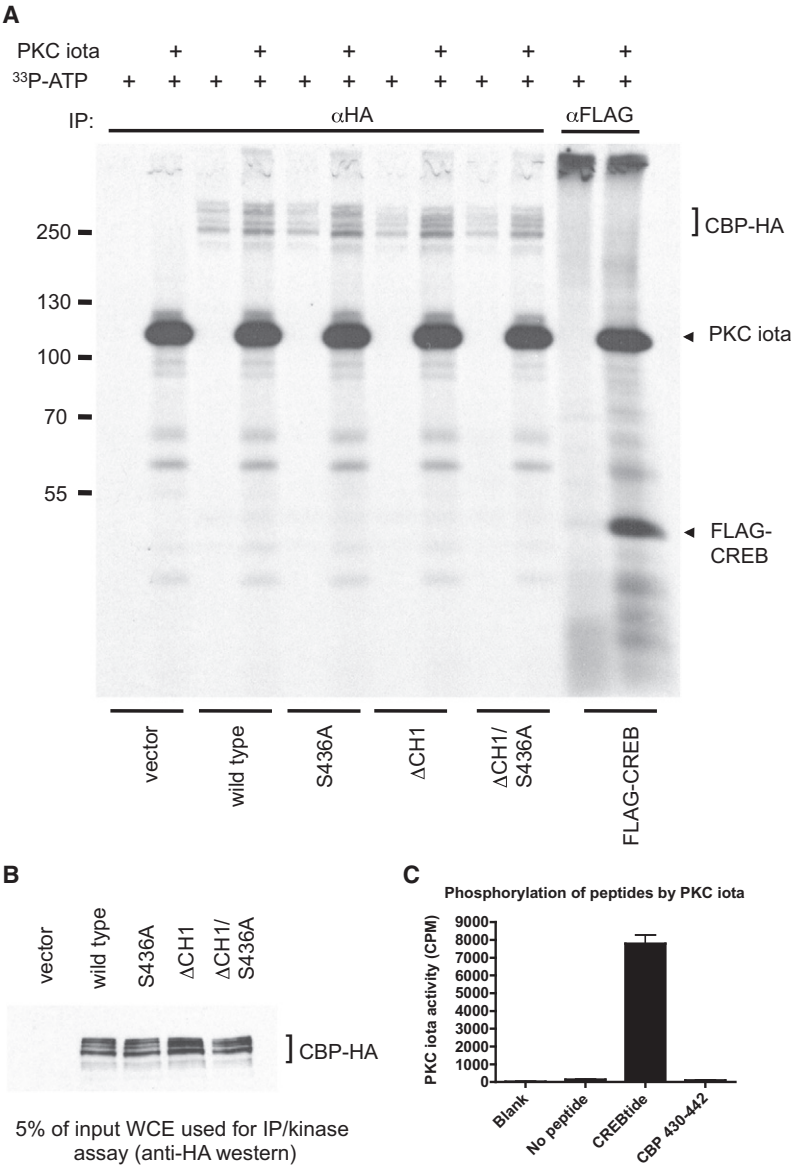

Figure 7. Purified Recombinant PKC Iota Does Not Efficiently Phosphorylate CBP Ser436 In Vitro

(A) SDS-PAGE autoradiogram following an in vitro kinase assay using 5 μM [^{33}P]-ATP, 0.1 μg PKC iota (indicated), and 293T whole-cell extract immunoprecipitates performed with anti-HA or anti-FLAG monoclonal antibodies. 293T cells were transiently transfected with the indicated expression vectors for CBP with an HA C-terminal epitope tag, empty vector, or CREB with a FLAG tag (positive control PKC substrate). The lower two bands of CBP-HA appear to lack the N-terminal region that includes the CH1 domain. Autophosphorylated PKC iota indicated.

(B) Western blot with anti-HA antibody shows 5% of input 293T extract used for IP kinase assay.

(C) In vitro kinase assays using synthetic peptides CREBtide, CBP 430–442, or water (no peptide). Data (c.p.m.) are from two independent experiments (n = 2–3), mean ± SEM). See also Figure S6.

et al., 2010; Xu et al., 2007). p300 is a prime HAT candidate to compensate for the loss of liver CBP, and analysis of CBP and p300 mRNA and protein levels in the liver suggests that the two coactivators are present in comparable amounts (Figures S1P–S1R) (Thorrez et al., 2008). The non-HAT CRTC2 may also provide functional redundancy, as it is limiting for the expression of certain CREB target genes in MEFs (Kasper et al., 2010), and for *Ppargc1a*, *Pck1*, and *G6pc* in the liver (Le Lay et al., 2009; Wang et al., 2010).

The metabolic functions of the CH1 domain are limiting, as mice heterozygous for the ΔCH1 mutation in *CBP* and *p300* tended to have intermediate phenotypes for adiposity and insulin sensitivity. Moreover, $p300^{\Delta CH1/\Delta CH1}$ mice resisted the weight gain, glucose intolerance, and insulin resistance associated with a HFD. These characteristics of the CH1 domain suggest that it would be a sensitive drug target for increasing metabolic control.

EXPERIMENTAL PROCEDURES

Animals

$CBP^{\Delta CH1}$, $p300^{\Delta CH1}$, and CBP^{flox} mice were previously described (Kang-Decker et al., 2004; Kasper et al., 2005). All studies used C57BL/6 X 129Sv F1 hybrid mice derived from congenic parents. F1 $p300^{\Delta CH1/\Delta CH1}$ mice were normal in appearance and had body lengths similar to WT animals, whereas adult $CBP^{\Delta CH1/\Delta CH1}$ mice were smaller and had moderate craniofacial anomalies (Kasper et al., 2005) (chiefly, blunt snouts, our unpublished data). All mice were used and cared for following protocols approved by the Institutional Animal Care and Use Committee of St. Jude.

Histology

Gonadal WAT pads were fixed with formaldehyde and stained with hematoxylin and eosin (H&E). ImageJ software was used to determine the number of cells for each of four random microscope fields of view for each of four serial sections cut ≥40 μM apart.

Cell Culture

$CBP^{\Delta CH1/\Delta CH1}$;$p300^{+/\Delta CH1}$ primary MEFs were described previously (Kasper et al., 2005). Differentiation of $CBP^{\Delta CH1/\Delta CH1}$;$p300^{+/\Delta CH1}$ and WT MEFs into adipocytes was carried out as described (Tanaka et al., 1997a), using Dulbecco's modified Eagle's medium (DMEM) supplemented with 10% heat-inactivated FBS, 0.5 mM IBMX, 1 μM dexamethasone, and 5 μg/ml insulin. This medium was renewed every other day for 12 days.

Metabolic Studies

Fasting blood glucose was measured by tail vein bleed and a Glucometer Elite (Bayer). GTT assays were performed on mice after a 16 hr overnight fast. Animals were injected i.p. with 20% D-glucose (2 mg/g body weight), and blood glucose was measured at the indicated times. ITT assays were carried out on mice fasted for 3 hr, injected i.p. with human insulin (0.75 IU /kg), and blood glucose measured at the indicated times. MTT assays were performed on mice fasted for 16 hr and injected i.p. with metformin (250 mg/kg) or saline vehicle. Human recombinant insulin (Humulin N, Lilly) was used as indicated for the animal experiments shown. Hepatic gene expression assays using WT mice injected with 0.75 IU/kg bovine insulin purchased from Sigma (I5500) yielded comparable results to Humulin N (data not shown).

High-Fat Diet Assays

Ten- to twelve-month-old male WT and $p300^{\Delta CH1/\Delta CH1}$ mice were fed a HFD ad libitum for 12 weeks (60% kcal from fat; Research Diets, NJ). Body weight

and food intake were monitored. GTT and ITT assays were performed (as described above) following 10 and 12 weeks, respectively, on the HFD. Serum triglycerides were measured using a kit (Sigma Catalog number TR0100) and serum from retro-orbital bleeds obtained 1 hr postprandial from anesthetized mice that had been fasted 16 hr overnight.

Cre-Mediated Deletion of *CBP*^{flox} in Liver

Mice were tail vein injected with 2.5 × 10^{10} genome copies of AAV-2/8-LP1-Cre (Cre expression driven by the liver-specific promoter of lipoprotein-1). Six days postinjection, male *CBP*$^{flox/flox}$ mice and WT controls (± AAV-Cre, as indicated) were fasted overnight for 16 hr before performing GTTs. Mice were then assessed for 6 hr fasting blood glucose, and then ITTs were performed, allowing 72 hr recovery intervals between assays. Finally, 96 hr following the ITT, mice were fasted overnight for assessment of 16 hr fasting blood glucose and then sacrificed to test hepatic gluconeogenic gene expression. Similar results for 16 hr fasting blood glucose and hepatic gluconeogenic gene expression were obtained 7 days after AAV-Cre infection for male and female *CBP*$^{flox/flox}$ mice (Figure S1). All mice within an experiment showed comparable inactivation of *CBP*^{flox} in the liver, as determined by semiquantitative PCR of genomic DNA (Kasper et al., 2006), qRT-PCR for WT *CBP* mRNA that contains exon 9 (the exon deleted by Cre-mediated recombination), and IP-western of CBP and p300 using equal volumes of liver nuclear extracts. IP assays were performed using pooled rabbit antisera raised against the N and C termini of CBP and p300. Western blots were performed using mouse monoclonal antibodies against CBP (C-1) or p300 (RW128).

Quantitative RT-PCR

Real-time reverse-transcription coupled PCR was performed as previously described (Xu et al., 2007). Samples were normalized to β-actin mRNA, and the expression levels for each test gene were set relative to the lowest value, which was defined as 1.

Liver ChIP

Mice were fasted for 16 hr overnight and after determination of fasting blood glucose were either injected i.p. with 0.5 IU/kg insulin, refed, or sacrificed as fasted controls. Blood glucose was also measured prior to sacrifice of the insulin-treated and refed mice. Whole-cell extracts for ChIP were prepared as described (Tuteja et al., 2008) using freshly dissected liver tissue treated for 10 min with 3% formaldehyde, followed by an equal volume of 2.5M glycine. ChIP assays were performed with extracts as described; qPCR ChIP signal was normalized to input chromatin (Kasper et al., 2005).

In Vitro Kinase Assays

In vitro phosphorylation of CBP-HA was carried out (as per the manufacturer's instructions) using 5 μM [^{33}P]-ATP and 0.1 μg PKC iota (Promega #V3751),and 293T whole-cell extract immunoprecipitates that had been washed sequentially with RIPA buffer (1% Nonidet P-40, 0.5% deoxycholate, 50 mM Tris [pH 7.5], 150 mM NaCl), 10 mM Tris (pH 7.5)/0.1% Nonidet P-40/300 mM NaCl, 10 mM Tris (pH 7.5)/0.1% Nonidet P-40/150 mM NaCl, and then 50 mM Tris (pH 7.5). Buffers contained protease inhibitors and β-glycerophosphate. Immunoprecipitations were performed with anti-HA or anti-FLAG monoclonal antibodies and protein G Sepharose. 293T cells were transiently transfected with expression vectors for mouse CBP with an HA C-terminal epitope tag, empty vector, or CREB with a FLAG tag (positive control PKC substrate). IP kinase reactions were incubated with shaking (600 RPM) for 30 min at 30°C. For kinase assays using the synthetic peptides CREBtide (KRREILSRRPSYR, a positive control, Promega) and CBP 430–442 (LPLKNASDKRNQQ), the reactions contained 7.5 μg peptide (~200 μM), 50 μM [^{33}P]-ATP, and 20 ng PKC iota in 25 μl and were incubated for 15 min at 30°C. Peptide reactions were terminated by drying 20 μl onto P81 phosphocellulose paper and then washing three times with 1% phosphoric acid.

Statistics

BMI was calculated as (weight [kg])/(body length [m])^2. Data are presented as mean ± standard error of the mean (SEM). Comparisons between groups were made by two-tailed t test or one-way analysis of variance (ANOVA) with Tukey or Dunnett's posttesting. Cumulative effects over time were measured by determining the area under the curve (AUC) using Graphpad Prism. $p > 0.05$ (not significant, N.S.), $^*p < 0.05$; $^{**}p < 0.01$ and $^{***}p < 0.001$.

SUPPLEMENTAL INFORMATION

Supplemental Information includes six figures and can be found with this article online at doi:10.1016/j.cmet.2011.06.010.

ACKNOWLEDGMENTS

We thank S. Lerach and T. Jeevan for excellent technical assistance; S. Jackowski, G. Oliver, and D. Green for access to equipment; and R. Leonard, M. Frank, M. Dillard, S. Tait, and S. Milasta for providing help and expertise. Thanks to these core facilities at St. Jude: Animal Resource Center, Animal Pathology, Biomedical Communications, and Vector Production and Development. The Hartwell Center at St. Jude provided oligonucleotides. This work was supported by National Institutes of Health grants DK058199 and DE018183 (P.K.B.), Cancer Center (CORE) support grant P30 CA021765, and the American Lebanese Syrian Associated Charities of St. Jude Children's Research Hospital.

Received: April 16, 2010
Revised: November 30, 2010
Accepted: June 9, 2011
Published: August 2, 2011

REFERENCES

Allis, C.D., Berger, S.L., Cote, J., Dent, S., Jenuwien, T., Kouzarides, T., Pillus, L., Reinberg, D., Shi, Y., Shiekhattar, R., et al. (2007). New nomenclature for chromatin-modifying enzymes. Cell *131*, 633–636.

Bedford, D.C., Kasper, L.H., Fukuyama, T., and Brindle, P.K. (2010). Target gene context influences the transcriptional requirement for the KAT3 family of CBP and p300 histone acetyltransferases. Epigenetics *5*, 9–15.

Biddinger, S.B., and Kahn, C.R. (2006). From mice to men: insights into the insulin resistance syndromes. Annu. Rev. Physiol. *68*, 123–158.

Brivet, M., Slama, A., Saudubray, J.M., Legrand, A., and Lemonnier, A. (1995). Rapid diagnosis of long chain and medium chain fatty acid oxidation disorders using lymphocytes. Ann. Clin. Biochem. *32*, 154–159.

Buzzai, M., Bauer, D.E., Jones, R.G., Deberardinis, R.J., Hatzivassiliou, G., Elstrom, R.L., and Thompson, C.B. (2005). The glucose dependence of Akt-transformed cells can be reversed by pharmacologic activation of fatty acid beta-oxidation. Oncogene *24*, 4165–4173.

Dames, S.A., Martinez-Yamout, M., De Guzman, R.N., Dyson, H.J., and Wright, P.E. (2002). Structural basis for Hif-1 alpha /CBP recognition in the cellular hypoxic response. Proc. Natl. Acad. Sci. USA *99*, 5271–5276.

De Guzman, R.N., Martinez-Yamout, M.A., Dyson, H.J., and Wright, P.E. (2004). Interaction of the TAZ1 domain of the CREB-binding protein with the activation domain of CITED2: regulation by competition between intrinsically unstructured ligands for non-identical binding sites. J. Biol. Chem. *279*, 3042–3049.

Feige, J.N., and Auwerx, J. (2007). Transcriptional coregulators in the control of energy homeostasis. Trends Cell Biol. *17*, 292–301.

Freedman, S.J., Sun, Z.Y., Poy, F., Kung, A.L., Livingston, D.M., Wagner, G., and Eck, M.J. (2002). Structural basis for recruitment of CBP/p300 by hypoxia-inducible factor-1 alpha. Proc. Natl. Acad. Sci. USA *99*, 5367–5372.

Freedman, S.J., Sun, Z.Y., Kung, A.L., France, D.S., Wagner, G., and Eck, M.J. (2003). Structural basis for negative regulation of hypoxia-inducible factor-1alpha by CITED2. Nat. Struct. Biol. *10*, 504–512.

Fujii, K., Zhu, G., Liu, Y., Hallam, J., Chen, L., Herrero, J., and Shaw, S. (2004). Kinase peptide specificity: improved determination and relevance to protein phosphorylation. Proc. Natl. Acad. Sci. USA *101*, 13744–13749.

Gu, J., Milligan, J., and Huang, L.E. (2001). Molecular mechanism of hypoxia-inducible factor 1alpha-p300 interaction. A leucine-rich interface regulated by a single cysteine. J. Biol. Chem. *276*, 3550–3554.

Halberg, N., Khan, T., Trujillo, M.E., Wernstedt-Asterholm, I., Attie, A.D., Sherwani, S., Wang, Z.V., Landskroner-Eiger, S., Dineen, S., Magalang, U.J., et al. (2009). Hypoxia-inducible factor 1alpha induces fibrosis and insulin resistance in white adipose tissue. Mol. Cell. Biol. *29*, 4467–4483.

He, L., Sabet, A., Djedjos, S., Miller, R., Sun, X., Hussain, M.A., Radovick, S., and Wondisford, F.E. (2009). Metformin and insulin suppress hepatic gluconeogenesis through phosphorylation of CREB binding protein. Cell *137*, 635–646.

Herzig, S., Long, F., Jhala, U.S., Hedrick, S., Quinn, R., Bauer, A., Rudolph, D., Schutz, G., Yoon, C., Puigserver, P., et al. (2001). CREB regulates hepatic gluconeogenesis through the coactivator PGC-1. Nature *413*, 179–183.

Hirschey, M.D., Shimazu, T., Goetzman, E., Jing, E., Schwer, B., Lombard, D.B., Grueter, C.A., Harris, C., Biddinger, S., Ilkayeva, O.R., et al. (2010). SIRT3 regulates mitochondrial fatty-acid oxidation by reversible enzyme deacetylation. Nature *464*, 121–125.

Kang-Decker, N., Tong, C., Boussouar, F., Baker, D.J., Xu, W., Leontovich, A.A., Taylor, W.R., Brindle, P.K., and Van Deursen, J.M. (2004). Loss of CBP causes T cell lymphomagenesis in synergy with p27(Kip1) insufficiency. Cancer Cell *5*, 177–189.

Kasper, L.H., and Brindle, P.K. (2006). Mammalian gene expression program resiliency: the roles of multiple coactivator mechanisms in hypoxia-responsive transcription. Cell Cycle *5*, 142–146.

Kasper, L.H., Boussouar, F., Ney, P.A., Jackson, C.W., Rehg, J., van Deursen, J.M., and Brindle, P.K. (2002). A transcription-factor-binding surface of coactivator p300 is required for haematopoiesis. Nature *419*, 738–743.

Kasper, L.H., Boussouar, F., Boyd, K., Xu, W., Biesen, M., Rehg, J., Baudino, T.A., Cleveland, J.L., and Brindle, P.K. (2005). Two transactivation mechanisms cooperate for the bulk of HIF-1-responsive gene expression. EMBO J. *24*, 3846–3858.

Kasper, L.H., Fukuyama, T., Biesen, M.A., Boussouar, F., Tong, C., de Pauw, A., Murray, P.J., van Deursen, J.M., and Brindle, P.K. (2006). Conditional knockout mice reveal distinct functions for the global transcriptional coactivators CBP and p300 in T-cell development. Mol. Cell. Biol. *26*, 789–809.

Kasper, L.H., Lerach, S., Wang, J., Wu, S., Jeevan, T., and Brindle, P.K. (2010). CBP/p300 double null cells reveal effect of coactivator level and diversity on CREB transactivation. EMBO J. *29*, 3660–3672.

Koo, S.H., Flechner, L., Qi, L., Zhang, X., Screaton, R.A., Jeffries, S., Hedrick, S., Xu, W., Boussouar, F., Brindle, P., et al. (2005). The CREB coactivator TORC2 is a key regulator of fasting glucose metabolism. Nature *437*, 1109–1114.

Kung, A.L., Rebel, V.I., Bronson, R.T., Ch'ng, L.E., Sieff, C.A., Livingston, D.M., and Yao, T.P. (2000). Gene dose-dependent control of hematopoiesis and hematologic tumor suppression by CBP. Genes Dev. *14*, 272–277.

Le Lay, J., Tuteja, G., White, P., Dhir, R., Ahima, R., and Kaestner, K.H. (2009). CRTC2 (TORC2) contributes to the transcriptional response to fasting in the liver but is not required for the maintenance of glucose homeostasis. Cell Metab. *10*, 55–62.

Lipina, C., Huang, X., Finlay, D., McManus, E.J., Alessi, D.R., and Sutherland, C. (2005). Analysis of hepatic gene transcription in mice expressing insulin-insensitive GSK3. Biochem. J. *392*, 633–639.

Marmorstein, R. (2001). Structure of histone acetyltransferases. J. Mol. Biol. *311*, 433–444.

Matsumoto, M., Ogawa, W., Akimoto, K., Inoue, H., Miyake, K., Furukawa, K., Hayashi, Y., Iguchi, H., Matsuki, Y., Hiramatsu, R., et al. (2003). PKClambda in liver mediates insulin-induced SREBP-1c expression and determines both hepatic lipid content and overall insulin sensitivity. J. Clin. Invest. *112*, 935–944.

Matt, T., Martinez-Yamout, M.A., Dyson, H.J., and Wright, P.E. (2004). The CBP/p300 TAZ1 domain in its native state is not a binding partner of MDM2. Biochem. J. *381*, 685–691.

Newton, A.L., Sharpe, B.K., Kwan, A., Mackay, J.P., and Crossley, M. (2000). The transactivation domain within cysteine/histidine-rich region 1 of CBP comprises two novel zinc-binding modules. J. Biol. Chem. *275*, 15128–15134.

Oike, Y., Hata, A., Mamiya, T., Kaname, T., Noda, Y., Suzuki, M., Yasue, H., Nabeshima, T., Araki, K., and Yamamura, K. (1999). Truncated CBP protein leads to classical Rubinstein-Taybi syndrome phenotypes in mice: implications for a dominant-negative mechanism. Hum. Mol. Genet. *8*, 387–396.

Ramnanan, C.J., Edgerton, D.S., Rivera, N., Irimia-Dominguez, J., Farmer, B., Neal, D.W., Lautz, M., Donahue, E.P., Meyer, C.M., Roach, P.J., and Cherrington, A.D. (2010). Molecular characterization of insulin-mediated suppression of hepatic glucose production in vivo. Diabetes *59*, 1302–1311.

Tanaka, T., Yoshida, N., Kishimoto, T., and Akira, S. (1997a). Defective adipocyte differentiation in mice lacking the C/EBPbeta and/or C/EBPdelta gene. EMBO J. *16*, 7432–7443.

Tanaka, Y., Naruse, I., Maekawa, T., Masuya, H., Shiroishi, T., and Ishii, S. (1997b). Abnormal skeletal patterning in embryos lacking a single Cbp allele: a partial similarity with Rubinstein-Taybi syndrome. Proc. Natl. Acad. Sci. USA *94*, 10215–10220.

Thorrez, L., Van Deun, K., Tranchevent, L.C., Van Lommel, L., Engelen, K., Marchal, K., Moreau, Y., Van Mechelen, I., and Schuit, F. (2008). Using ribosomal protein genes as reference: a tale of caution. PLoS ONE *3*, e1854. 10.1371/journal.pone.0001854.

Tilghman, S.M., Hanson, R.W., Reshef, L., Hopgood, M.F., and Ballard, F.J. (1974). Rapid loss of translatable messenger RNA of phosphoenolpyruvate carboxykinase during glucose repression in liver. Proc. Natl. Acad. Sci. USA *71*, 1304–1308.

Tuteja, G., Jensen, S.T., White, P., and Kaestner, K.H. (2008). Cis-regulatory modules in the mammalian liver: composition depends on strength of Foxa2 consensus site. Nucleic Acids Res. *36*, 4149–4157.

Wang, Y., Inoue, H., Ravnskjaer, K., Viste, K., Miller, N., Liu, Y., Hedrick, S., Vera, L., and Montminy, M. (2010). Targeted disruption of the CREB coactivator Crtc2 increases insulin sensitivity. Proc. Natl. Acad. Sci. USA *107*, 3087–3092.

Xu, W., Kasper, L.H., Lerach, S., Jeevan, T., and Brindle, P.K. (2007). Individual CREB-target genes dictate usage of distinct cAMP-responsive coactivation mechanisms. EMBO J. *26*, 2890–2903.

Yamauchi, T., Oike, Y., Kamon, J., Waki, H., Komeda, K., Tsuchida, A., Date, Y., Li, M.X., Miki, H., Akanuma, Y., et al. (2002). Increased insulin sensitivity despite lipodystrophy in Crebbp heterozygous mice. Nat. Genet. *30*, 221–226.

Yao, T.P., Oh, S.P., Fuchs, M., Zhou, N.D., Ch'ng, L.E., Newsome, D., Bronson, R.T., Li, E., Livingston, D.M., and Eckner, R. (1998). Gene dosage-dependent embryonic development and proliferation defects in mice lacking the transcriptional integrator p300. Cell *93*, 361–372.

Yu, J., and Auwerx, J. (2009). The role of sirtuins in the control of metabolic homeostasis. Ann. N Y Acad. Sci. *1173* (*Suppl 1*), E10–E19.

Zanger, K., Radovick, S., and Wondisford, F.E. (2001). CREB binding protein recruitment to the transcription complex requires growth factor-dependent phosphorylation of its GF box. Mol. Cell *7*, 551–558.

Zhang, X., Lam, K.S., Ye, H., Chung, S.K., Zhou, M., Wang, Y., and Xu, A. (2010). Adipose tissue-specific inhibition of hypoxia inducible factor 1{alpha} induces obesity and glucose intolerance by impeding energy expenditure in mice. J. Biol. Chem. *285*, 32869–32877.

Zhao, S., Xu, W., Jiang, W., Yu, W., Lin, Y., Zhang, T., Yao, J., Zhou, L., Zeng, Y., Li, H., et al. (2010). Regulation of cellular metabolism by protein lysine acetylation. Science *327*, 1000–1004.

Zhou, X.Y., Shibusawa, N., Naik, K., Porras, D., Temple, K., Ou, H., Kaihara, K., Roe, M.W., Brady, M.J., and Wondisford, F.E. (2004). Insulin regulation of hepatic gluconeogenesis through phosphorylation of CREB-binding protein. Nat. Med. *10*, 633–637.